

Skyrme nuclear energy density functionals from atomic nuclei to neutron stars

Nicolas Chamel

in collaboration with S. Goriely, J. M. Pearson and
A. F. Fantina

Institute of Astronomy and Astrophysics
Université Libre de Bruxelles, Belgium



KITPC, June 2012

Outline

- 1 Atomic mass models based on Skyrme nuclear energy density functionals
 - ▷ pairing
 - ▷ spin-isospin instabilities
 - ▷ self-interactions
 - ▷ neutron-matter stiffness

- 2 Applications of Skyrme functionals to neutron stars

Why do we need new Skyrme functionals ?



The interpretation of many astrophysical phenomena requires the knowledge of nuclear properties which are not experimentally accessible and won't be measured in a near future

Effective nuclear energy density functional

- **In principle, one can construct the nuclear functional from realistic NN forces** (i.e. fitted to experimental NN phase shifts) using many-body methods

$$\mathcal{E} = \frac{\hbar^2}{2M}(\tau_n + \tau_p) + A(\rho_n, \rho_p) + B(\rho_n, \rho_p)\tau_n + B(\rho_p, \rho_n)\tau_p$$

$$+ C(\rho_n, \rho_p)(\nabla \rho_n)^2 + C(\rho_p, \rho_n)(\nabla \rho_p)^2 + D(\rho_n, \rho_p)(\nabla \rho_n) \cdot (\nabla \rho_p)$$

+ Coulomb, spin-orbit and pairing

Drut, Furnstahl and Platter, Prog. Part. Nucl. Phys. 64(2010)120.

- **But this is a very difficult task** so in practice, we construct phenomenological (Skyrme) functionals
Bender, Heenen and Reinhard, Rev. Mod. Phys. 75, 121 (2003).

Why not using existing Skyrme functionals?

Most of existing Skyrme functionals are not suitable for astrophysics.

- They were adjusted to a few selected nuclei (mostly in the stability valley)
→ not suited for investigating stellar nucleosynthesis.
- They were not fitted to the neutron-matter EoS
→ not suited for neutron-star studies.

It is difficult to get physical insight on how to optimize the functional because each one was constructed using a different fitting procedure.

Construction of the functional

Experimental data:

- 2149 atomic masses with $Z, N \geq 8$ from 2003 AME
- compressibility $230 \leq K_v \leq 250$ MeV
- charge radius of ^{208}Pb , $R_c = 5.501 \pm 0.001$ fm
- symmetry energy $J = 30$ MeV

N-body calculations with realistic forces:

- isoscalar effective mass $M_s^*/M = 0.8$
- equation of state of pure neutron matter
- 1S_0 pairing gaps in symmetric and neutron matter
- Landau parameters, stability against spurious spin and spin-isospin instabilities

Phenomenological corrections for atomic nuclei

For atomic nuclei, we add the following corrections

- Wigner energy

$$E_W = V_W \exp \left\{ -\lambda \left(\frac{N-Z}{A} \right)^2 \right\} + V'_W |N-Z| \exp \left\{ -\left(\frac{A}{A_0} \right)^2 \right\}$$

$$V_W \sim -2 \text{ MeV}, V'_W \sim 1 \text{ MeV}, \lambda \sim 300 \text{ MeV}, A_0 \sim 20$$

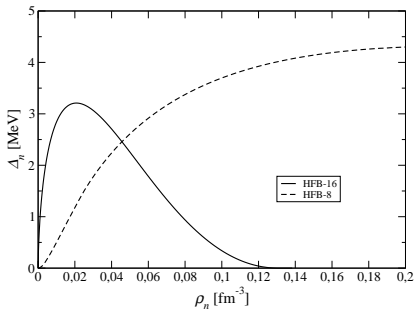
- rotational and vibrational spurious collective energy

$$E_{\text{coll}} = E_{\text{rot}}^{\text{crank}} \left\{ b \tanh(c|\beta_2|) + d|\beta_2| \exp\{-l(|\beta_2| - \beta_2^0)^2\} \right\}$$

In this way, these collective effects do not contaminate the parameters of the functional.

Pairing functional

Local pairing energy density functionals



The pairing EDF is very poorly constrained by fitting pairing gaps in nuclei. Other observables are required to pinpoint the density and isospin dependence of the pairing strength.

Chamel, Goriely, Pearson, Nucl. Phys.A812,72 (2008).

Instead, the pairing EDF is assumed to be *locally* the same as in homogeneous matter.

Garrido et al., Phys.Rev.C60,064312(1999).

Margueron, Sagawa&Hagino, Phys.Rev.C77,054309(2008).

Empirical pairing energy density functionals

The pairing functional is generally parametrized as

$$\mathcal{E}_{\text{pair}} = \frac{1}{4} \sum_{q=n,p} v^{\pi q}[\rho_n, \rho_p] \tilde{\rho}_q^2$$

$$v^{\pi q}[\rho_n, \rho_p] = V_{\pi q}^{\Lambda} \left(1 - \eta_q \left(\frac{\rho_n + \rho_p}{\rho_0} \right)^{\alpha q} \right)$$

This functional has to be supplemented with a cutoff prescription.

Drawbacks

- not enough flexibility to fit realistic pairing gaps in infinite nuclear matter and in finite nuclei (\Rightarrow isospin dependence)
- the global fit to nuclear masses would be computationally very expensive

Pairing in nuclei and in nuclear matter

$v^{\pi q}[\rho_n, \rho_p] = v^{\pi q}[\Delta_q(\rho_n, \rho_p)]$ constructed so as to reproduce *exactly* a realistic gap $\Delta_q(\rho_n, \rho_p)$ in homogeneous matter

Inverting the HFB equations in homogeneous matter yields

$$v^{\pi q} = -8\pi^2 \left(\frac{\hbar^2}{2M_q^*} \right)^{3/2} \left(\int_{\Lambda} \frac{\sqrt{\varepsilon} d\varepsilon}{\sqrt{(\varepsilon - \mu_q)^2 + \Delta_q(\rho_n, \rho_p)^2}} \right)^{-1}$$

Chamel, Goriely, Pearson, Nucl. Phys.A812,72 (2008).

- **one-to-one correspondence** between pairing in nuclei and nuclear matter
- **no free parameters**
- **automatic renormalization** of the pairing strength with ε_{Λ}

Analytical expression of the pairing strength

Integrating the gap equation can be numerically costly for global mass fits. But in the “weak-coupling approximation” $\Delta_q \ll \mu_q$ and $\Delta_q \ll \varepsilon_\Lambda$

$$v^{\pi q} \simeq -\frac{8\pi^2}{\sqrt{\mu_q}} \left(\frac{\hbar^2}{2M_q^*} \right)^{3/2} \left[2 \log \left(\frac{2\mu_q}{\Delta_q} \right) + \Lambda \left(\frac{\varepsilon_\Lambda}{\mu_q} \right) \right]^{-1}$$

$$\Lambda(x) = \log(16x) + 2\sqrt{1+x} - 2 \log \left(1 + \sqrt{1+x} \right) - 4$$

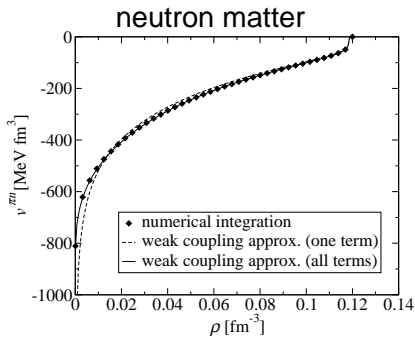
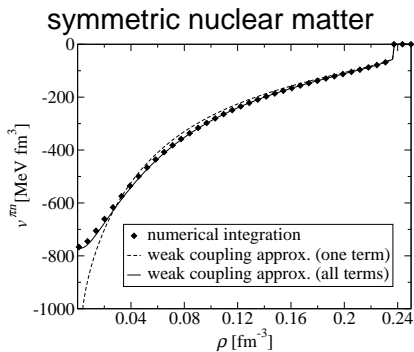
s.p. energy cutoff ε_Λ above the Fermi level

Chamel, Phys. Rev. C 82, 014313 (2010)

This expression is as easy to numerically implement as empirical functionals

Accuracy of the weak-coupling approximation

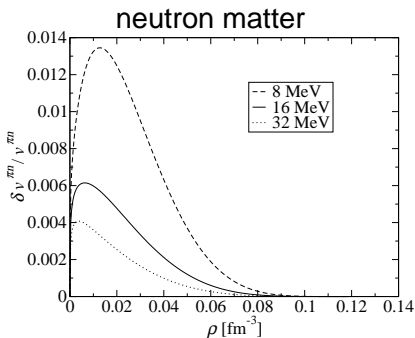
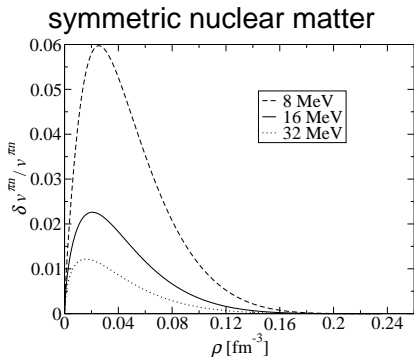
This approximation remains **very accurate at low densities** because the s.p. density of states is not replaced by a constant as in the usual “weak-coupling approximation”.



Chamel, *Phys. Rev. C* 82, 014313 (2010)

Accuracy of the weak-coupling approximation

This approximation remains **very accurate at low densities** because the s.p. density of states is not replaced by a constant as in the usual “weak-coupling approximation”.



Chamel, *Phys. Rev. C* 82, 014313 (2010)

Pairing cutoff and experimental phase shifts

In the limit of vanishing density, the pairing strength

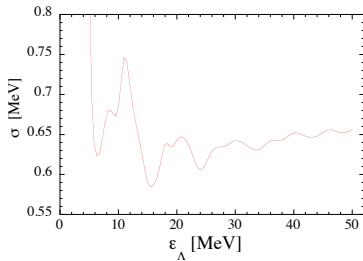
$$v^{\pi q}[\rho \rightarrow 0] = -\frac{4\pi^q}{\sqrt{\varepsilon_\Lambda}} \left(\frac{\hbar^2}{2M_q} \right)^{3/2}$$

should coincide with the bare force in the 1S_0 channel.

A fit to the **experimental 1S_0 NN phase shifts** yields

$\varepsilon_\Lambda \sim 7 - 8$ MeV.

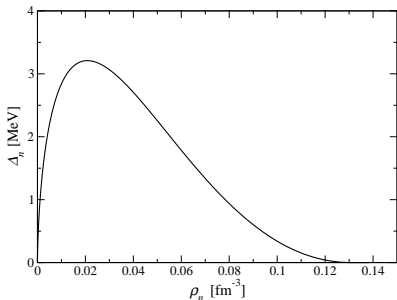
Esbensen et al., Phys. Rev. C 56, 3054 (1997).



On the other hand, a better mass fit can be obtained with $\varepsilon_\Lambda \sim 16$ MeV
Goriely et al., Nucl.Phys.A773(2006),279.
Chamel et al., arXiv:1204.2076

Choice of the pairing gap

Fit the 1S_0 pairing gap obtained with realistic NN potentials at the BCS level



1S_0 pairing gaps in neutron matter obtained with Argonne V14 potential

- $\Delta_n(\rho_n)$ essentially independent of the NN potential
- $\Delta_n(\rho_n)$ completely determined by experimental 1S_0 nn phase shifts

Dean&Hjorth-Jensen, Rev.Mod.Phys.75(2003)607.

Other contributions to pairing

In order to take into account

- Coulomb and charge symmetry breaking effects
- polarization effects in odd nuclei (we use the equal filling approximation)
- coupling to surface vibrations

we introduce renormalization factors f_q^\pm ($f_n^+ \equiv 1$ by definition)

$$v^{\pi n} \longrightarrow f_n^\pm v^{\pi n}$$

$$v^{\pi p} \longrightarrow f_p^\pm v^{\pi p}$$

Typically $f_q^\pm \simeq 1 - 1.2$

HFB-16 mass table

Results of the fit on the 2149 measured masses with $Z, N \geq 8$ from the 2003 Atomic Mass Evaluation

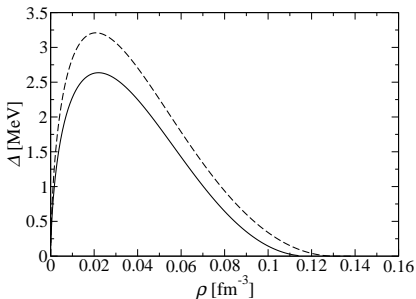
	HFB-16	FRDM
$\sigma(M)$ [MeV]	0.632	0.656
$\bar{\epsilon}(M)$ [MeV]	-0.001	0.058
$\sigma(M_{nr})$ [MeV]	0.748	0.919
$\bar{\epsilon}(M_{nr})$ [MeV]	0.161	0.047
$\sigma(S_n)$ [MeV]	0.500	0.399
$\bar{\epsilon}(S_n)$ [MeV]	-0.012	-0.001
$\sigma(Q_\beta)$ [MeV]	0.559	0.498
$\bar{\epsilon}(Q_\beta)$ [MeV]	0.031	0.004
$\sigma(R_C)$ [fm]	0.0313	0.0545
$\bar{\epsilon}(R_C)$ [fm]	-0.0149	-0.0366

Chamel, Goriely, Pearson, Nucl. Phys.A812,72 (2008).

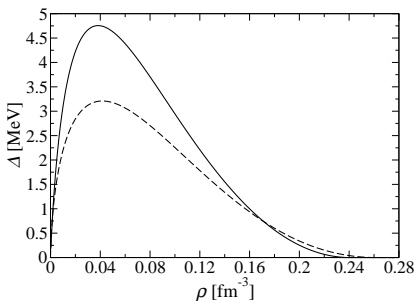
HFB-17 mass model: microscopic pairing gaps including medium polarization effects

Fit the 1S_0 pairing gaps of both neutron matter and symmetric nuclear matter obtained from **Brueckner calculations taking into account medium polarization effects**

Neutron matter



Symmetric nuclear matter



Cao et al., *Phys.Rev.C*74,064301(2006).

HFB-17 mass table

Results of the fit on the 2149 measured masses with $Z, N \geq 8$ from the 2003 Atomic Mass Evaluation

	HFB-16	HFB-17
$\sigma(2149 M)$	0.632	0.581
$\bar{\epsilon}(2149 M)$	-0.001	-0.019
$\sigma(M_{nr})$	0.748	0.729
$\bar{\epsilon}(M_{nr})$	0.161	0.119
$\sigma(S_n)$	0.500	0.506
$\bar{\epsilon}(S_n)$	-0.012	-0.010
$\sigma(Q_\beta)$	0.559	0.583
$\bar{\epsilon}(Q_\beta)$	0.031	0.022
$\sigma(R_c)$	0.0313	0.0300
$\bar{\epsilon}(R_c)$	-0.0149	-0.0114
$\theta(^{208}\text{Pb})$	0.15	0.15

Goriely, Chamel, Pearson, *PRL* 102, 152503 (2009).

Predictions of HFB vs newly measured atomic masses

HFB mass models were fitted to the 2003 Atomic Mass Evaluation. How reliable are these models?

The predictions of these models are in good agreement with new mass measurements

	HFB-16	HFB-17
$\sigma(434 M)$	0.484	0.363
$\bar{\epsilon}(434 M)$	-0.136	-0.092
$\sigma(142 M)$	0.516	0.548
$\bar{\epsilon}(142 M)$	-0.070	0.172

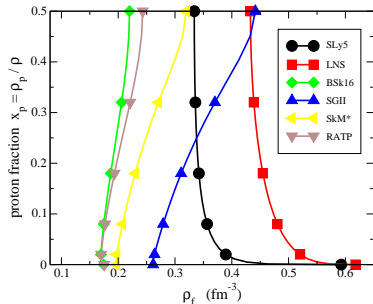
Litvinov et al., Nucl.Phys.A756, 3(2005)

http://research.jyu.fi/igisol/JYFLTRAP_masses/gs_masses.txt

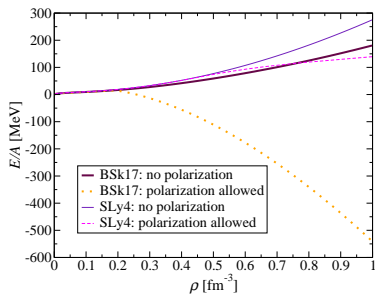
Spin-isospin instabilities

Ferromagnetic instability

Unlike microscopic calculations, conventional Skyrme functionals predict a ferromagnetic transition in nuclear matter sometimes leading to a ferromagnetic collapse of neutron stars.



Margueron et al.,
J.Phys.G36(2009),125102.



Chamel et al.,
Phys.Rev.C80(2009),065804.

Spin stability in symmetric nuclear matter restored

The ferromagnetic instability can be completely removed by including the **density-dependent** term in the Skyrme force

$$t_5(1 + x_5 P_\sigma) \frac{1}{\hbar^2} \mathbf{p}_{ij} \cdot \rho(\mathbf{r})^\beta \delta(\mathbf{r}_{ij}) \mathbf{p}_{ij}$$

Problem: this new term will also change the nuclear properties at low densities! Introduce another force of the form

$$\frac{1}{2} t_4(1 + x_4 P_\sigma) \frac{1}{\hbar^2} \left\{ \mathbf{p}_{ij}^2 \rho(\mathbf{r})^\beta \delta(\mathbf{r}_{ij}) + \delta(\mathbf{r}_{ij}) \rho(\mathbf{r})^\beta \mathbf{p}_{ij}^2 \right\}$$

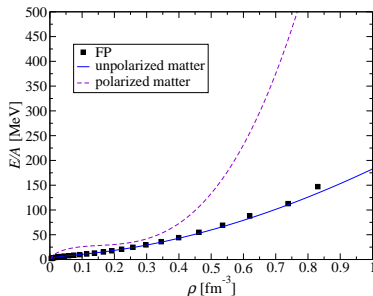
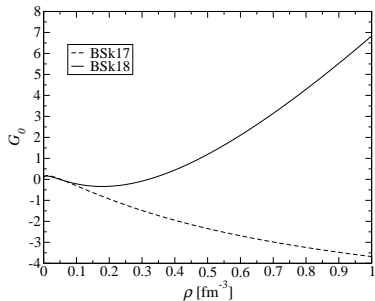
The t_4 and t_5 terms exactly cancel in unpolarized nuclear matter (for any isospin asymmetry) provided

$$t_4(1 - x_4) = -3t_5(1 + x_5), \quad x_4(5 + 4x_5) = -(4 + 5x_5)$$

Chamel, Goriely, Pearson, Phys.Rev.C80(2009),065804.

Spin stability in asymmetric nuclear matter restored

With t_4 and t_5 terms, the ferromagnetic instability is completely removed not only in symmetric nuclear matter but also in neutron matter for any spin polarization.



We have checked that no instabilities arise in neutron stars at any densities.

Chamel, Goriely, Pearson, Phys.Rev.C80(2009),065804.

HFB-18 mass model

Results of the fit on the 2149 measured masses with $Z, N \geq 8$

	HFB-18	HFB-17
$\sigma(M)$ [MeV]	0.585	0.581
$\bar{\epsilon}(M)$ [MeV]	0.007	-0.019
$\sigma(M_{nr})$ [MeV]	0.758	0.729
$\bar{\epsilon}(M_{nr})$ [MeV]	0.172	0.119
$\sigma(S_n)$ [MeV]	0.487	0.506
$\bar{\epsilon}(S_n)$ [MeV]	-0.012	-0.010
$\sigma(Q_\beta)$ [MeV]	0.561	0.583
$\bar{\epsilon}(Q_\beta)$ [MeV]	0.025	0.022
$\sigma(R_c)$ [fm]	0.0274	0.0300
$\bar{\epsilon}(R_c)$ [fm]	0.0016	-0.0114
$\theta(^{208}\text{Pb})$ [fm]	0.15	0.15

HFB-18 yields almost identical results as HFB-17 for nuclei

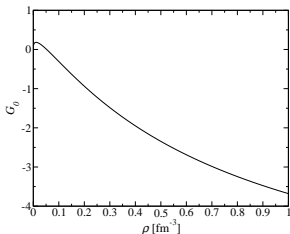
Spin and spin-isospin instabilities

Although HFB-18 yields stable neutron-star matter, it still predicts spurious spin-isospin instabilities in symmetric matter.

Spurious spin and spin-isospin instabilities arise from the C_0^T and C_1^T terms in the Skyrme functional:

$$\mathcal{E}_{\text{Sky}}^{\text{pol}} = \mathcal{E}_{\text{Sky}}^{\text{unpol}} + C_0^s \mathbf{s}^2 + C_1^s (\mathbf{s}_n - \mathbf{s}_p)^2 + C_0^T \mathbf{s} \cdot \mathbf{T} + C_1^T (\mathbf{s}_n - \mathbf{s}_p) \cdot (\mathbf{T}_n - \mathbf{T}_p)$$

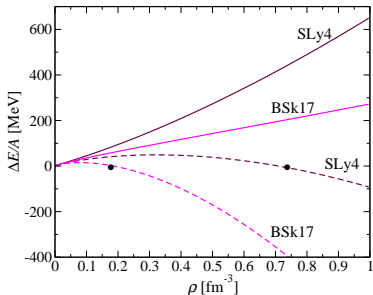
with $\mathbf{s}_q = \rho_{q\uparrow} - \rho_{q\downarrow}$ and $\mathbf{T}_q = \tau_{q\uparrow} - \tau_{q\downarrow}$.



In symmetric matter, the ferromagnetic stability is governed by the Landau parameter $G_0 = 2N_0(C_0^s + C_0^T k_F^2)$.

Spin-isospin instabilities

- Setting $C_t^T > 0$ remove spin-isospin instabilities but can lead to instabilities in nuclei.
- All instabilities (at any temperature and degree of polarization) can be removed by setting $C_t^T = 0$, which means dropping J^2 terms due to gauge invariance.



Difference between the energy per particle in fully polarized neutron matter and in unpolarized neutron matter with (dashed line) and without (solid line) C_t^T terms.

Chamel&Goriely, Phys.Rev.C82, 045804 (2010)

Landau parameters and the J^2 terms

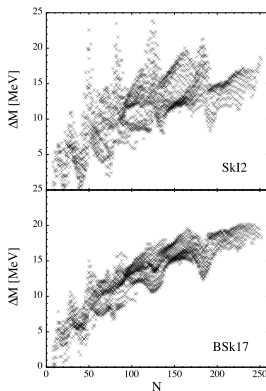
Landau parameters for selected Skyrme forces which were fitted without the J^2 terms. Values in parenthesis were obtained by setting $C_t^T = 0$.

	G_0	G'_0	G_0^{NeuM}
SGII	0.01 (0.62)	0.51 (0.93)	-0.07 (1.19)
SLy4	1.11 (1.39)	-0.13 (0.90)	0.11 (1.27)
SkI1	-8.74 (1.09)	3.17 (0.90)	-5.57 (1.10)
SkI2	-1.18 (1.35)	0.77 (0.90)	-1.08 (1.24)
SkI3	0.57 (1.90)	0.20 (0.85)	-0.19 (1.35)
SkI4	-2.81 (1.77)	1.38 (0.88)	-2.03 (1.40)
SkI5	0.28 (1.79)	0.30 (0.85)	-0.31 (1.30)
SkO	-4.08 (0.48)	1.61 (0.98)	-3.17 (0.97)
LNS	0.83 (0.32)	0.14 (0.92)	0.59 (0.91)
Microscopic	0.83	1.22	0.77

Impact of the J^2 terms

Dropping the J^2 terms and their associated time-odd parts

- removes spin and spin-isospin instabilities at any $T \geq 0$
- prevents an anomalous behavior of the entropy
- improves the values of Landau parameters (especially G'_0) and the sum rules.



Warning:

Adding or removing a posteriori the J^2 terms without refitting the functional can induce large errors!

Chamel & Goriely, Phys.Rev.C82, 045804 (2010)

More about the J^2 terms

On the other hand dropping the J^2 terms leads to

- unrealistic effective masses in polarized matter

$$\frac{\hbar^2}{2M_{q\sigma}^*} = \frac{\hbar^2}{2M_q^*} \pm \left[s(C_0^T - C_1^T) + 2s_q C_1^T \right] \Rightarrow M_{q\uparrow}^* = M_{q\downarrow}^* = M_q^*$$

- self-interaction errors.

Instabilities can be removed *with* the J^2 terms by adding density-dependent terms in C_0^T and C_1^T (t_4 and t_5 terms). But only for zero temperature.

Chamel, Goriely, Pearson, Phys.Rev.C80(2009),065804.

Self-interactions

Self-interactions

In the one-particle limit, the potential energy obtained from phenomenological functionals may not vanish.

Considering the most general semi-local functional with all possible bilinear terms up to 2nd order in the derivatives

$$\begin{aligned}\mathcal{E}_{\text{Sky}} = & \sum_{t=0,1} C_t^\rho \rho_t^2 + C_t^{\Delta\rho} \rho_t \Delta\rho_t + C_t^T \rho_t \tau_t + C_t^{\nabla J} \rho_t \nabla \cdot \mathbf{J}_t \\ & + C_t^J \sum_{\mu,\nu} J_{t,\mu\nu} J_{t,\mu\nu} + \frac{1}{2} C_t^{TrJ} \left(\sum_{\mu} J_{t,\mu\mu} \right)^2 + \frac{1}{2} C_t^{J^2} \sum_{\mu,\nu} J_{t,\mu\nu} J_{t,\nu\mu} \\ & + C_t^s s_t^2 + C_t^{\Delta s} \mathbf{s}_t \cdot \Delta \mathbf{s}_t + C_t^T \mathbf{s}_t \cdot \mathbf{T}_t + C_t^{j_t^2} j_t^2 + C_t^{\nabla j} \mathbf{s}_t \cdot \nabla \times \mathbf{j}_t \\ & + C_t^{\nabla s} (\nabla \cdot \mathbf{s}_t)^2 + C_t^F \mathbf{s}_t \cdot \mathbf{F}_t\end{aligned}$$

Removal of self-interactions

Requiring the cancellation of self-interactions leads to the fundamental constraints

$$C_0^\rho + C_1^\rho + C_0^s + C_1^s = 0$$

$$C_0^\tau + C_1^\tau + C_0^T + C_1^T = 4(C_0^{\Delta\rho} + C_1^{\Delta\rho} + C_0^{\Delta s} + C_1^{\Delta s})$$

$$4(C_0^{\nabla s} + C_1^{\nabla s}) + C_0^F + C_1^F = 0$$

$$C_0^\tau + C_1^\tau - 2(C_0^T + C_1^T) - (C_0^F + C_1^F) - 4(C_0^{\Delta s} + C_1^{\Delta s}) = 0$$

Chamel, Phys. Rev. C 82, 061307(R) (2010).

Self-interaction errors

Self-interaction errors in the one-particle limit can contaminate systems consisting of many particles.

For instance, in polarized neutron matter the error in the energy density caused by self-interactions is given by

$$\delta \mathcal{E}_{\text{NeuM}}^{\text{pol}} = (C_0^\rho + C_1^\rho + C_0^s + C_1^s) \rho^2$$

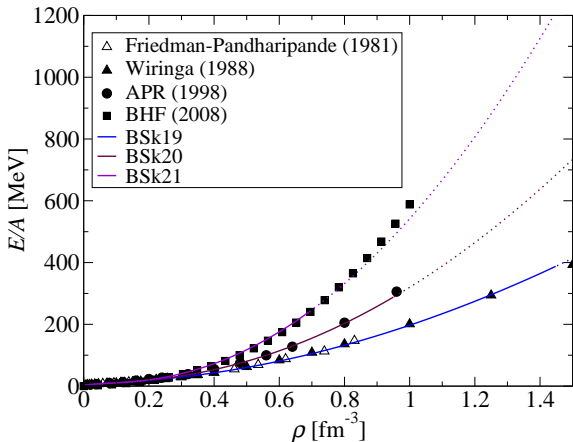
If $C_0^\rho + C_1^\rho + C_0^s + C_1^s < 0$, self-interactions would thus drive a ferromagnetic collapse of neutron stars.

The use of effective forces prevent *one-particle* self-interaction errors but not necessarily *many-body* self-interaction errors (e.g. t_3 term).

Neutron-matter stiffness

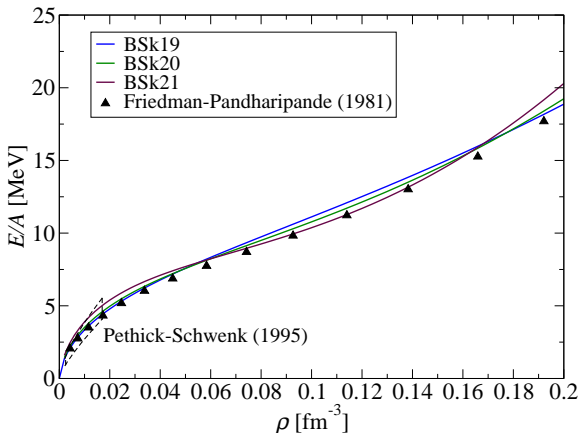
Neutron-matter equation of state at high densities

We have recently constructed a family of three different generalized Skyrme functionals BSk19, BSk20 and BSk21 (with t_4 and t_5) spanning the range of realistic neutron-matter equations of state at high densities.



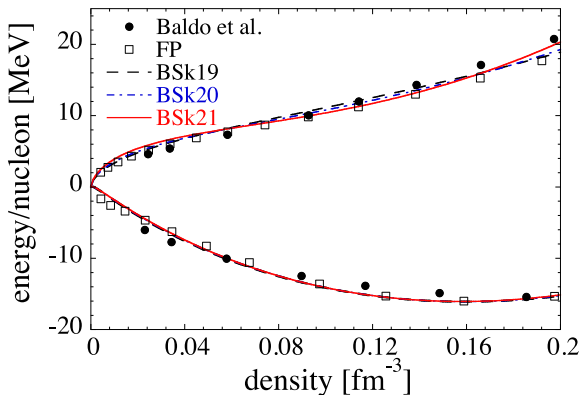
Neutron-matter equation of state at low densities

All three functionals yield similar neutron-matter equations of state at subsaturation densities consistent with microscopic calculations using realistic NN interactions



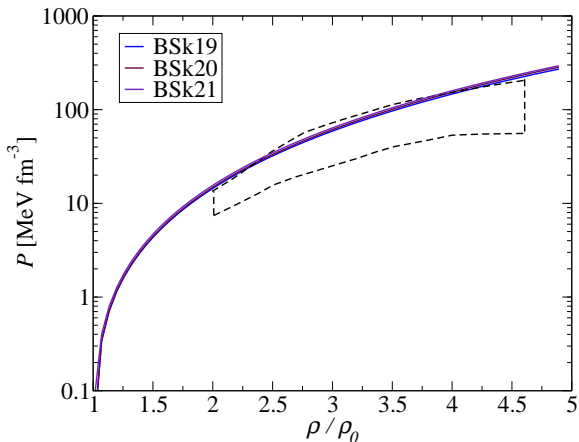
Nuclear-matter equation of state

Our functionals (which were only fitted to neutron matter) are also in excellent agreement with BHF calculations in symmetric nuclear matter.



Constraints from heavy-ion collisions

Our functionals are consistent with the pressure of symmetric nuclear matter inferred from Au+Au collisions

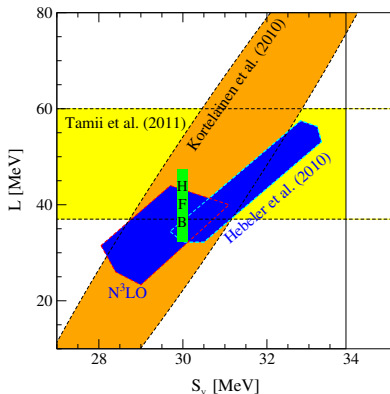


Danielewicz et al., Science 298, 1592 (2002).

Symmetry energy

Our functionals are consistent with chiral EFT calculations and ^{208}Pb polarizability measurement.

Tews, Krueger, Hebeler, Schwenk, arXiv:1206.0025.



Effective masses

Our functionals predict a qualitatively correct splitting of effective masses ($M_n^* > M_p^*$ in neutron-rich matter) in agreement with giant resonances and many-body calculations using realistic forces.

$$\frac{M}{M_q^*} = \frac{2\rho_q}{\rho} \frac{M}{M_s^*} + \left(1 - \frac{2\rho_q}{\rho}\right) \frac{M}{M_v^*}$$

	BSk19	BSk20	BSk21	EBHF
M_s^*/M	0.80	0.80	0.80	0.825
M_v^*/M	0.61	0.65	0.71	0.727

BSk21 is also in good **quantitative agreement** with Extended Brueckner Hartree-Fock (EBHF) calculations.

Cao et al., Phys.Rev.C73,014313(2006).

HFB-19, HFB-20 and HFB-21 mass tables

Results of the fit on the 2149 measured masses with $Z, N \geq 8$ from the 2003 Atomic Mass Evaluation

<http://www.astro.ulb.ac.be/bruslib/>

	HFB-19	HFB-20	HFB-21	HFB-18
$\sigma(M)$ [MeV]	0.583	0.583	0.577	0.585
$\bar{\epsilon}(M)$ [MeV]	-0.038	0.021	-0.054	0.007
$\sigma(M_{nr})$ [MeV]	0.803	0.790	0.762	0.758
$\bar{\epsilon}(M_{nr})$ [MeV]	0.243	0.217	-0.086	0.172
$\sigma(S_n)$ [MeV]	0.502	0.525	0.532	0.487
$\bar{\epsilon}(S_n)$ [MeV]	-0.015	-0.012	-0.009	-0.012
$\sigma(Q_\beta)$ [MeV]	0.612	0.620	0.620	0.561
$\bar{\epsilon}(Q_\beta)$ [MeV]	0.027	0.024	0.000	0.025
$\sigma(R_C)$ [fm]	0.0283	0.0274	0.0270	0.0274
$\bar{\epsilon}(R_C)$ [fm]	-0.0032	0.0009	-0.0014	0.0016
$\theta(^{208}\text{Pb})$ [fm]	0.140	0.140	0.137	0.150

Goriely, Chamel, Pearson, *Phys.Rev.C*82,035804(2010).

Comparison with the latest experimental data

The latest experimental data from the 2011 AME favor HFB-21.

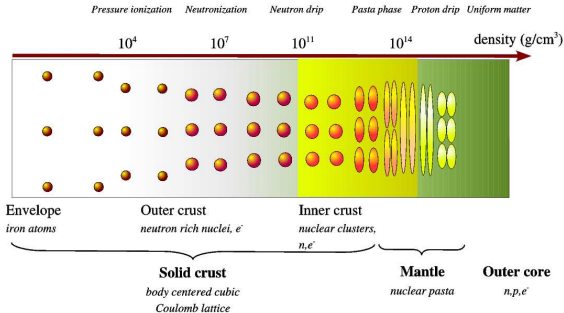
<http://www-nds.iaea.org/amdc/>

	$\bar{\epsilon}(M)$ [MeV]	$\sigma(M)$ [MeV]
HFB-21	-0.031	0.574
HFB-20	-0.010	0.595
HFB-19	0.051	0.593
HFB-18	0.026	0.582
HFB-17	0.0008	0.581
FRDM	0.062	0.645

Applications to neutron stars

Internal constitution of neutron stars

The EDF theory is well-suited for describing the **very different phases of matter** found in the interior of neutron stars.



Chamel&Haensel, *Living Reviews in Relativity* 11 (2008), 10
<http://relativity.livingreviews.org/Articles/lrr-2008-10/>

Unified equation of state of a neutron star

The EDF theory allows for a unified treatment of all regions of a neutron star.

- **outer crust** (nuclei+relativistic electron gas)
BPS model with HFB mass table
Pearson, Goriely and Chamel, Phys.Rev.C 83,065810(2011).
- **inner crust** (clusters+neutron gas+relativistic electron gas)
Extended Thomas-Fermi+proton shell correction
Pearson, Goriely, Chamel, Ducoin, Phys.Rev.C85,065803(2012).
- **core** (neutrons+protons+leptons)

Composition of the outer crust of a neutron star

Sequence of equilibrium nuclides with increasing depth:

HFB-19	HFB-20	HFB-21
⁵⁶ Fe	⁵⁶ Fe	⁵⁶ Fe
⁶² Ni	⁶² Ni	⁶² Ni
⁶⁴ Ni	⁶⁴ Ni	⁶⁴ Ni
⁶⁶ Ni	⁶⁶ Ni	⁶⁶ Ni
⁸⁶ Kr	⁸⁶ Kr	⁸⁶ Kr
⁸⁴ Se	⁸⁴ Se	⁸⁴ Se
⁸² Ge	⁸² Ge	⁸² Ge
⁸⁰ Zn	⁸⁰ Zn	⁸⁰ Zn
⁸² Zn	⁸² Zn	-
-	-	⁷⁹ Cu
-	⁷⁸ Ni	⁷⁸ Ni
⁸⁰ Ni	⁸⁰ Ni	⁸⁰ Ni
¹²⁶ Ru	¹²⁶ Ru	-
¹²⁴ Mo	¹²⁴ Mo	¹²⁴ Mo
-	¹²² Mo	-
¹²² Zr	¹²² Zr	¹²² Zr
¹²⁴ Zr	¹²⁴ Zr	-
-	-	¹²¹ Y
¹²⁰ Sr	¹²⁰ Sr	¹²⁰ Sr
¹²² Sr	¹²² Sr	¹²² Sr
¹²⁴ Sr	¹²⁴ Sr	¹²⁴ Sr
¹²⁶ Sr	¹²⁶ Sr	-

The first 8 nuclides are completely determined by experimental atomic masses.

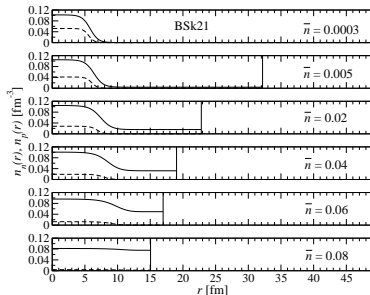
Deeper in the crust the composition is more model-dependent. Measurements of neutron-rich nuclei are crucially needed.
Pearson, Goriely, Chamel, Phys. Rev. C83, 065810.

Structure of the inner crust of a neutron star

With increasing density, the clusters keep essentially the same size but become more and more dilute:

Crust-core transition properties

	\bar{n}_{cc} (fm^{-3})	P_{cc} (MeV fm^{-3})
BSk19	0.0885	0.428
BSk20	0.0854	0.365
BSk21	0.0809	0.268
SLy4	0.0798	0.361

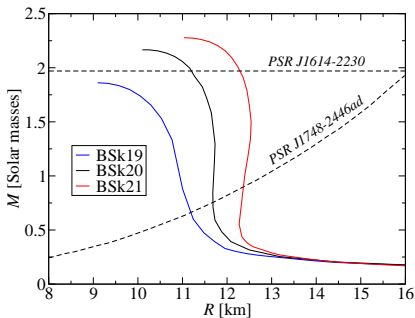
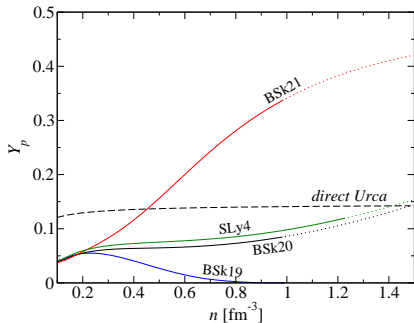


Note that HFB-19-20-21 all predict a neutron-skin thickness of 0.14 in ^{208}Pb .

The crust-core transition is found to be very smooth: the crust dissolves continuously into a uniform mixture of neutrons, protons and electrons

Unified equation of state of neutron stars

All regions of a neutron star are described using the same functional.



Neutron star observations rule out the softest of our EoS and favor BSk21 since direct Urca should occur in some stars.

Chamel et al., Phys.Rev.C84,062802(2012).

Summary

We have developed Skyrme functionals for HFB atomic mass models and for neutron stars:

- they give an excellent fit to essentially all experimental mass data ($\sigma \lesssim 0.6$ MeV)
- they give an excellent fit to other properties of finite nuclei such as charge radii ($\sigma \lesssim 0.03$ fm)
- they also reproduce various properties of homogeneous nuclear matter (EoS, 1S_0 pairing gaps, effective masses)
- they do not contain spurious spin-isospin instabilities in homogeneous nuclear matter

Both the latest experimental atomic mass data and astrophysical observations favor HFB-21.